HEFAT2008
6th International Conference on Heat Transfer, Fluid Mechanics and Thermodynamics
30 June to 2 July 2008
Pretoria, South Africa
Paper number: AF1

A NUMERICAL INVESTIGATION OF GAS INJECTION INTO A CYLINDER FILLED WITH CASTOR OIL USING THE TWO-FLUID MODEL

Farshad Abbasi *, Hasan Rahimzadeh, Seyed Emad Hoseini
*Author for correspondence
Department of Mechanical Engineering,
Islamic Azad University of Marivan,
Marivan,
I.R.IRAN,
E-mail: farshadmit@yahoo.com

ABSTRACT

An Eulerian-Eulerian two-fluid mathematical model is used to numerical simulation of two-phase flow caused by the gas injection into a vertical cylinder. The cylinder is filled with castor oil of which the kinematics viscosity is sufficiently large to ensure liquid flow to be in the laminar regime. The mathematical model used in this study, solves transport equations for the variables of each phase with an allowance for interphase mass and momentum exchange. The governing equations are discreted by the finite volume technique and then are solved by *SIMPLE* staggered grid solution technique. In order to increase the accuracy of calculations, the *power-law* scheme is employed to approximate the convection and diffusion terms. It is found that the radial components of bubbles velocities are much smaller than the corresponding axial ones, and the bubbles move up almost vertically. Predictions of the proposed model agree closely with a number of published experimental data.

INTRODUCTION

Bubbly flows are central to many industrial and natural processes, such as bubble columns, gas absorption, oxidation processes, hydrogen production, chlorate process, electroplating, metal purification, etc. In order to enhance the rate of transport between the phases in many direct contact heat and/or mass exchange processes, a condensable gas is often injected into a liquid through a submerged orifice or nozzle. Despite the extensive application of this basic flow phenomenon, the design of these systems has been mainly based on trial and empirical methods. Hence, a detail examination on the mass, momentum and energy transfer is essential for improving and optimizing the design of such industrial processes. However, due to the complexity of two-phase flow systems, standard formulation of the governing equations for bubble-driven flow has not yet been established. The theoretical models in literature usually considered the gas-liquid mixture as a single fluid with variable density caused by the distribution of bubbles in liquid. In addition, since the properties of two-fluids are combined into those of one mixture, this model cannot be used to predict the flow behavior of each phase. In the present state-of-the-art, the two-fluid model can be considered as the most detailed and accurate macroscopic formulation of the two-phase flow systems.

NOMENCLATURE

C_d	[-]	drag coefficient
D	[m^2/s]	diffusion coefficient
d_b	[m]	bubble diameter
F_r	[kg/m^2s^2]	volumetric inter-fluid friction
Re	[-]	Reynolds number
v	[m/s]	r-velocity vector
w	[m/s]	z-velocity vector
F_b	[kg/m^2s^2]	buoyancy forces
g	m/s^2]	gravity vector
H	[m]	height of cylinder
R	[m]	radius of cylinder
A	[$1/m$]	interfacial area per unit volume
N	[$1/m^3$]	number of bubbles per unit volume
Greek letters		
α	[-]	volume fraction ratio
ρ	[kg/m^3]	density
μ	[$N.s/m^2$]	viscosity
Subscripts		
b		bubble
g		gas phase
l		liquid phase
eff		effective

There are extensive studies available in the literature investigating mass transfer and flow mechanisms in two-phase flow systems. In the recent study of Sherman et al [1] a two-fluid model coupled with population balance approach is used to numerical simulation of bubbly flow in a vertical isothermal channel. Durst et al [2] performed experimental studies on bubble-driven laminar flows by investigating liquid circulation and bubble's street with Laser-Doppler system. In their experiments, the flow was established in a glass cylinder of 100 mm i.d. with bubbles generated at a 0.5 mm dia. nozzle located at the centre of the bottom wall of container and the cylinder was filled with castor oil. Air was passed through a well-controlled pressure regulator and the resulting bubbles left the nozzles at a steady rate of one for every 0.55 s with diameter db of about 5.0-6.5 mm. Two depths of liquid (H=0.098 m and H=0.278 m) were investigated to determine the profiles of liquid and bubble velocities. Durst et al [3] also conducted numerical simulations on the bubble-driven flows at which both the single-phase model and the two-fluid model were used. In the two-fluid model, momentum equations for the liquid phase were derived from the Navier-Stokes equation, while equations for the gas-phase were simplified by neglecting the viscous forces. Celik and Wang [4] used a modified drift-flux model to simulate the problem with the same operating parameters as the experiments by Durst et al [2]. It was reported that the liquid-phase circulation pattern is not sensitive to the actual shape of the void fraction profiles. Detailed predictions on the liquid phase are given in their studies, while the corresponding ones for gas phase are not complete. Johansen et al [5] studied the fluid dynamics in bubble-stirred ladles by employing a Laser-Doppler system to measure the axial and radial mean velocities of liquid phase. Air was supplied through a porous plug placed in the bottom wall of a cylindrical Perspex-water model of a ladle. However, no measurement on the gas phase was conducted. Johansen and Boysan [6] proposed a mathematical model to describe the fluid flow in the bubble-stirred ladle at which Eulerian and Lagrangian methods were used to analyse the liquid and gas phases, respectively. A limited number of comparisons were conducted between simulations and experimental results of the liquid phase, but no information on the gas phase was reported. Castillejos and Brimacombe [7] studied the plume formation and liquid circulation induced by gas injection at the bottom of cylindrical water containers. They developed an electro-resistivity probe to measure the detailed bubble characteristics such as gas volume fraction, bubble velocity and size. In addition, the axial and radial components of the liquid velocity surrounding the plume were measured by means of a Laser-Doppler system.

In the present study, we use a two-fluid mathematical model, including the effects of inter-phase mass and momentum transfer, to numerical simulation of steady-state gas injection into a vertical cylinder. In addition, we use the same operating parameters as the experiments by Durst et al [2] and Celik et al [4].

PHYSICAL SETTING AND MATHEMATICAL MODEL

The schematic sketch of problem considered is given in Fig. 1. In this figure, r and z represents the radial and axial coordinates, respectively. v and w stand for the velocity components in radial and axial directions, respectively. In such a system, gas is injected into a liquid bath (with a depth of H and a diameter of R) from an orifice located at the bottom wall of a cylindrical vessel at a steady state flow rate. The actual dimensions of the liquid container and gas injection rates are specified according to the available experimental data of Durst et al [2] and Celik et al [4]. The configuration parameters for the simulation are listed in Table 1.

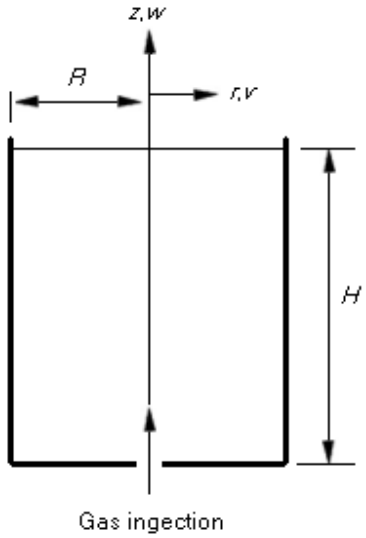

Fig. 1. Schematic diagram of problem.

The zone-averaged quantities are obtained through the solution of separate transport equations for each phase. Within this framework, the governing equations for the steady-state; two-phase flow system can be expressed in cylindrical coordinates and conservative form as follows:

Table 1. Physical configuration for the laminar bubble-driven flow [2,4].

Radius of container (R)	0.1 m	Bubble diameter (d_b)	6×10^{-3} m
Liquid depth (H)	0.098 m	Gas injection rate (Q)	2.6×10^{-7} m^3/s
Density of liquid (ρ_l)	960.3 kg/m^3	Gas density (ρ_g)	1.29 kg/m^3
Viscosity of liquid (μ_l)	0.6712 N s/m^2	Viscosity of gas (μ_g)	1.64×10^{-5} N s/m^2

MASS CONSERVATION

$$\frac{\partial}{\partial t}(\alpha_i\rho_i)+\frac{\partial}{\partial r}(\rho_i\alpha_i v_i)+\frac{\partial}{\partial z}(\rho_i\alpha_i w_i)+ \frac{\rho_i\alpha_i v_i}{r}=M_{i-\text{int}}, \quad (1)$$

where subscript, *i* represents the phases and takes the value of *l, g* in this problem. The term in the right hand of this equation represents the diffusion of one phase to the other phase.

R-MOMENTUM

$$\frac{\partial}{\partial t}(\rho_i\alpha_i v_i)+\frac{\partial}{\partial r}(\rho_i\alpha_i v_i^2)+\frac{\partial}{\partial z}(\rho_i\alpha_i v_i w_i)= -\frac{\partial}{\partial r}(p\alpha_i)+F_r(v_j-v_i)+\frac{\partial}{\partial r}(\alpha_i\mu_{eff_i}\frac{\partial v_i}{\partial r})+ \frac{\partial}{\partial z}(\alpha_i\mu_{eff_i}\frac{\partial v_i}{\partial z})+\alpha_i\mu_{eff_i}(\frac{1}{r}\frac{\partial v_i}{\partial r}-\frac{v_i}{r^2}), \quad (2)$$

Z-MOMENTUM

$$\frac{\partial}{\partial t}(\rho_i\alpha_i w_i)+\frac{\partial}{\partial r}(\rho_i\alpha_i v_i w_i)+\frac{\partial}{\partial z}(\rho_i\alpha_i w_i^2)= -\frac{\partial}{\partial z}(p\alpha_i)+F_r(w_j-w_i)+\rho_i\alpha_i g+\frac{\partial}{\partial r}(\alpha_i\mu_{eff_i}\frac{\partial w_i}{\partial r})+ \frac{\partial}{\partial z}(\alpha_i\mu_{eff_i}\frac{\partial w_i}{\partial z})+\alpha_i\mu_{eff_i}(\frac{1}{r}\frac{\partial w}{\partial z}), \quad (3)$$

F_r in both momentum equations is interface friction term and represents momentum exchange between the phases per unit volume and $F_b=\rho g$ is the buoyancy force where g is the gravity vector.

AUXILIARY EQUATIONS

Mass diffusion between the two phases at the gas–liquid interface, $M_{i-\text{int}}$ is calculated as:

$$M_{i-\text{int}}=\frac{\partial}{\partial r}(\rho_i D_i\frac{\partial\alpha_i}{\partial r})+\frac{\partial}{\partial z}(\rho_i D_i\frac{\partial\alpha_i}{\partial z})+ \frac{\rho_i D_i}{r}\frac{\partial\alpha_i}{\partial r}, \quad (4)$$

where D_i represents mass diffusion coefficient of phase *i* .

Interface friction term, F_r in momentum equations can be expressed as:

$$F_r=\frac{1}{8}C_d A_{\text{lg}}\alpha_l\frac{\mu_l}{d_b}\text{Re}_b, \quad (5)$$

where C_d , A_{lg} represent the drag coefficient and interfacial area per unit volume, respectively. Assuming that bubbles have a spherical shape with a characteristic diameter of d_b , the drag coefficient is given by [8]:

$$C_d=\frac{24.0}{\text{Re}_b}(1+0.15\,\text{Re}_b^{0.687})+\frac{0.42}{(1+\frac{42500}{\text{Re}_b^{1.16}})}, \quad (6)$$

where Re_b is the Reynolds number based on the gas bubble diameter:

$$\text{Re}_b=\frac{\rho_l\left|U_l-U_g\right|d_b}{\mu_l}, \quad (7)$$

where $\left|U_l-U_g\right|$ is the slip velocity vector between the two phases.

The interfacial area concentration A_{lg} is related to the gas void fraction α_g and the bubble diameter d_b as follow [9,10]:

$$A_{\text{lg}}=\frac{6\alpha_g}{d_b}, \quad (8)$$

NUMERICAL METHOD

The finite volume method is employed to discrete the governing equations. A staggered grid is adopted to obtain a compact stencil for pressure. On the staggered grids, the flow properties such as volume fraction, density and pressure are located at the center of the main control volume. The whole set of equations is solved by incorporating the *SIMPLE* algorithm of Patankar and Spalding [11]. Because of the nonlinearity of the governing equations and the coupling of variables, iterative numerical procedures are conducted until the convergence is reached.

SENSITIVITY ANALYSIS: INFLUENCE OF GRID ARRANGEMENT

Prior to evaluating the models, the influence of grid density on the precision of numerical results was analyzed. Therefore, a two-dimensional computational domain was built and three different grid arrangements (8×16, 24×16, 32×16 uniform rectangular cells) were tested. It is found that there is no significant difference between the predicted results of the 24×16 and the 32×16 grid arrangements. Therefore it is confirmed that the 24×16 grid arrangement is adequate to the problem of the present study.

RESULTS AND DISCUSSIONS

The predicted results include the gas distribution and velocity field for both the liquid and gas phases, comparing with the experimental data's of Durst et al [2].

The predicted axial bubble velocity along the centerline of vessel (normalized by the maximum bubble axial velocity $w_{g,\max}$) is shown in Fig. 2. Reasonable agreement is seen between the predictions and experimental results. Near the gas entrance, the bubbles are driven by the buoyancy force and move upwards. After a certain distance from the leading point, bubbles reach a terminal velocity and move up at this speed until they reach the vicinity of the free surface where the bubble velocities are reduced due to the increase of drag force caused by increasing relative motion between the bubble and liquid phases. It should be noted that because of natural convection the liquid flow is a result of friction between two phases. Therefore, when the liquid approaches the free surface, the

axial velocity decreases while the radial velocity increases. As a result, the liquid shifts in the radial direction and causes the liquid circulation in the container.

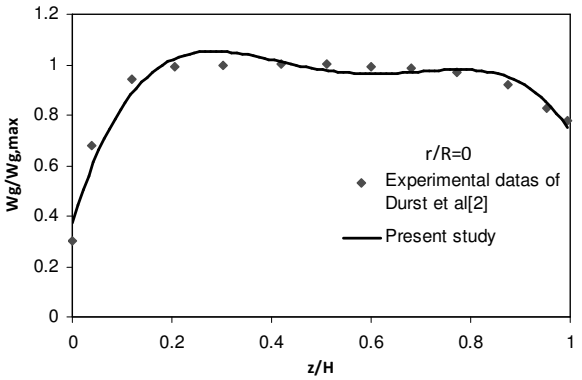

Fig. 2. Gas phase axial velocity along the centerline of vessel.

Fig. 3 shows the comparison between the predicted profiles of axial liquid velocity (normalized by the maximum bubble axial velocity) and the experimental results, at the vertical section of (*z/H*=0.36). It is seen that the maximum liquid velocity is located on the centerline of the plume where the maximum gas volume fraction is formed. The significant decrease of axial liquid velocity along the lateral direction may be attributed to the decrease of bubble void fraction due to the weakness of bubble diffusion. Our simulation is in reasonable agreements with the experimental results.

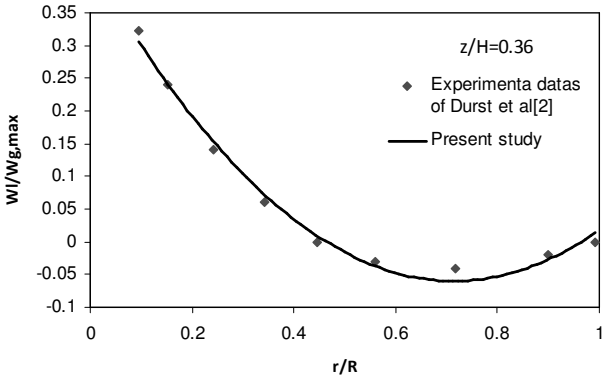

Fig. 3. Predicted vertical component of liquid velocity at the vertical section of *z/H*=0.36.

The predicted gas void fraction profiles at two vertical sections in the cylinder are presented in Figs. 4 and 5. It is seen that the maximum gas volume fraction is located in the centre of the container. Most of the bubbles are located in the central region of the container, and bubble volume fraction near the gas injection orifice is higher than that far away from the orifice. The significant decrease of gas void fraction along the lateral direction of cylinder may be attributed to the decrease of bubble diffusion. It is seen that the predicted gas void fraction agrees closely with the experimental data's.

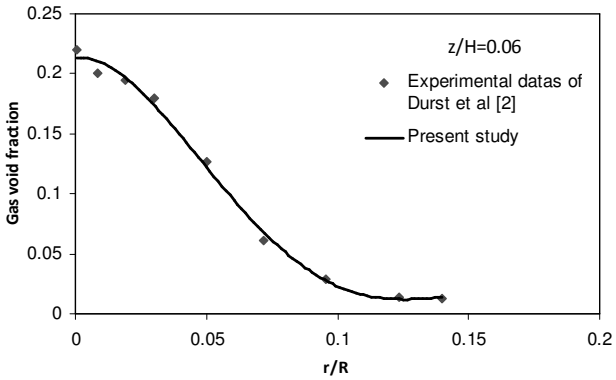

Fig. 4. Predicted gas void fraction distribution at the vertical section of *z/H*=0.06.

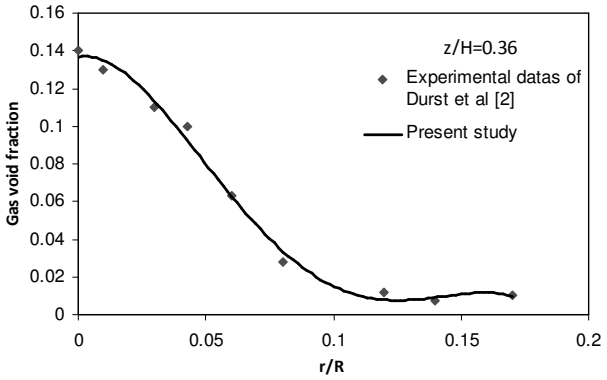

Fig. 5. Predicted gas void fraction distribution at the vertical section of *z/H*=0.36.

Interfacial area and bubble numbers profiles predicted by the present model could not be directly compared with those measured by Durst et al [2] as they did not present these data. Fig.6 shows interfacial area profile predicted using Eq. (8). As shown, interfacial area concentration is increasing toward to the top of the container because of buoyancy and convection of bubbles along the container.

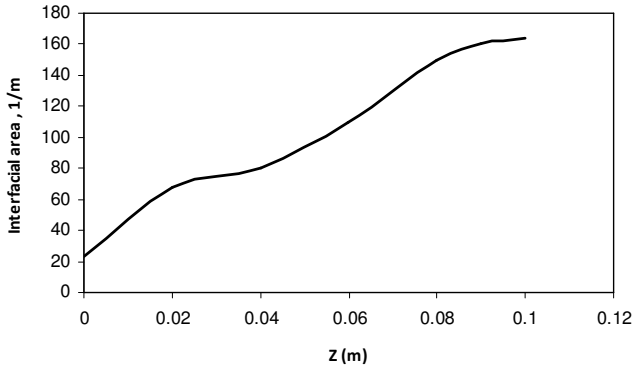

Fig. 6. Predicted interfacial area concentration along the container.

Fig. 7 shows the distribution of bubble numbers per unit volume along the container. The number of bubbles per unit volume N_b is calculated as:

$$N_b = \frac{6\alpha_g}{\pi d_b^3}, \quad (9)$$

It is seen that, the number of bubbles increases along the container. This increase is attributed to the accumulation of bubbles towards the top of the container due to buoyancy.

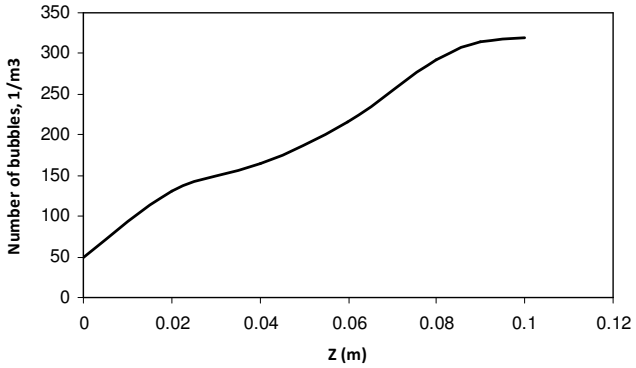

Fig. 7. Predicted distribution of bubble numbers along the container.

CONCLUSION

Gas injection into a vertical cylinder filled with castor oil, is investigated numerically using an Eulerian-Eulerian two-fluid mathematical model. The predicted results achieve a satisfactory agreement with the experimental data in the literature. The main conclusions rising from the present study are as follows:

1) Most of the bubbles are located in the central region of the container, and bubble volume fraction near the gas injection orifice is higher than that far away from the orifice.
2) The maximum liquid velocity is located on the centerline of the plume where the maximum gas volume fraction is formed.
3) The radial components of bubbles velocities are much smaller than the corresponding axial ones, and the bubbles move up almost vertically.
4) The decrease of axial liquid velocity at the vicinity of the free surface causes the liquid circulation in the container.

REFERENCES

[1] Sherman C.P. Cheung, G.H. Yeoh, J.Y. Tu, On the modeling of population balance in isothermal vertical bubbly flows-Average bubble number density approach, *International journal of Chemical Engineering and Processing*, 2007, 46, 742–756.

[2] Durst F., Taylor A. M. K. P., Whitelaw J. H., Experimental and numerical investigation of bubble-driven laminar flow in an axisymmetric vessel, *International Journal of Multiphase Flow*, 1984, 10, 557-569.

[3] Durst F., Schonung B., Selanger K., Winter M, Bubble-driven liquid flows, *Journal of Fluid Mechanics,* 1986, 170, 53-82.

[4] Celik I., Wang Y. Z, Numerical simulation of circulation in gas-liquid column reactor: isothermal, bubbly, laminar flow, *International Journal of Multiphase Flow,* 1994, 20, 1053-1070.

[5] Johansen S. T., Robertson D. G. C., Woje K., Engh T. A., Fluid dynamics in bubble stirred ladles: Part I. Experiments., *Metallurgical Transactions*, 1988, 19B, 745-754.

[6] Johansen S. T., Boysan F., Fluid dynamics in bubble stirred ladles: Part II: Mathematical modeling, *Metallurgical Transactions*, 1988, 19B, 755-764.

[7] Castillejos A. H., Brimacombe J. K., Measurements of physical characteristics of bubbles in gas-liquid plumes: Part II: Local properties of turbulent air-water plumes in vertically injected jets. *Metallurgical Transactions*, 1987, 18B, 659-671.

[8] Simonin O. et al, Eulerian prediction of the fluid/particle correlated motion in turbulent two-phase flows, *Applied Scientific Research*, 1993, 51, 275.

[9] X. Li, R. Wang, R. Huang, Y. Shi, Numerical investigation of boiling flow of nitrogen in a vertical tube using the two-fluid model, *Applied Thermal Engineering*, 2006, 26, 2425–2432.

[10] J.Y.Tu, G.H.Yeoh., On Numerical Modelling of Low-Pressure Subcooled Boiling Flow, *International Journal of Heat and Mass Transfer*, 2002, 45, 1197-1209.

[11] Patankar S. V., Spalding D. B., A calculation procedure for heat, mass and momentum transfer in three-dimensional parabolic flows, *International Journal of Heat Mass Transfer*, 1972, 15, 1787-1806.